

# Parametric weight reduction design study of a small-diameter axial bearing for automotive tie rod applications

Sinan Dayı , Mehmet Çevik\* 

Department of Mechanical Engineering, İzmir Katip Çelebi University, İzmir 35620, Türkiye

\* **Corresponding author:** Mehmet Çevik, [mehmet.cevik@ikcu.edu.tr](mailto:mehmet.cevik@ikcu.edu.tr)

## CITATION

Dayı S, Çevik, M. Parametric weight reduction design study of a small-diameter axial bearing for automotive tie rod applications. *Mechanical Engineering Advances*. 2025; 3(4): 3818.  
<https://doi.org/10.59400/mea3818>

## ARTICLE INFO

Received: 25 July 2025  
Revised: 2 September 2025  
Accepted: 6 September 2025  
Available online: 2 October 2025

## COPYRIGHT



Copyright © 2025 Author(s).  
*Mechanical Engineering Advances* is published by Academic Publishing Pte. Ltd. This work is licensed under the Creative Commons Attribution (CC BY) license.  
<https://creativecommons.org/licenses/by/4.0/>

**Abstract:** Reducing component mass in automotive steering systems is a key strategy for achieving energy consumption reduction, cost efficiency, and sustainability, provided that functional safety and durability are preserved. This study experimentally investigates the feasibility of reducing the inner tie rod ball diameter from Ø29 mm to Ø26 mm while maintaining compliance with functional and durability requirements. Unlike predominantly simulation-driven studies, an industrial, hands-on experimental methodology is employed under realistic production conditions. A total of 192 inner tie rod assemblies were manufactured, comprising a Ø29 mm reference configuration and multiple Ø26 mm variants produced by systematically varying pressing force, tempering method, and tempering temperature. All assemblies were first subjected to functional screening based on articulation torque, axial travel, and minimum axial stiffness. Only configurations satisfying all acceptance criteria were advanced to wear and setting durability tests. Each assembly was evaluated using repeated measurements, and results are reported as mean values with corresponding standard deviations. The results show that articulation torque is the most sensitive parameter in reduced-diameter designs and is strongly influenced by tempering strategy and press force. Combining ball tempering with an increased press force provided stable functional behavior before and after both wear and setting tests, satisfying all acceptance criteria. The validated Ø26 mm configuration enables an estimated 10% weight reduction, approximately 8% material-related cost savings, and associated energy consumption reduction without introducing additional manufacturing steps. The findings deliver production-ready guidance for lightweight inner tie rod design while meeting stringent automotive safety standards.

**Keywords:** energy efficiency; parametric design; tempering; automotive applications; articulation torque

## 1. Introduction

The evolution of automotive steering systems, from basic mechanical setups to complex, power-assisted designs like rack and pinion, has highlighted the critical role of tie rods in vehicle safety and performance. Tie rods, which transmit steering input from the steering rack to the wheels, consist of two parts (inner and outer) connected by a threaded joint, allowing for precise steering alignment and vehicle handling. Despite advancements in steering technology, tie rods remain fundamental to controlling vehicle movement. **Figure 1** illustrates the components of the inner tie rod assembly.

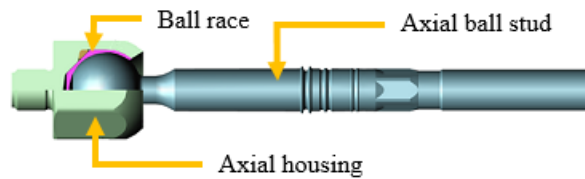


**Figure 1.** Inner tie rod components.

Tie rods, critical to a vehicle's steering mechanism, endure significant forces during operation, leading to wear, particularly in the plastic bearings within their ball joints, which facilitate horizontal and vertical movement. Ensuring durability is vital for safety, as tie rods are designed to fail before more expensive components like the steering gear or knuckle sustain damage.

Inner tie rods are manufactured from cold-forged steel and consist of three main components: a ball stud, housing, and plastic bearing. Manufacturing considerations include using high-strength materials like steel or heat-treated aluminum to balance strength, weight, and cost while meeting global standards such as AK-LH 14, 2014 [1]. Testing and design account for variable forces from different road conditions, ensuring performance across smooth and rough terrains.

Previous research on tie rod and ball joint assemblies has emphasized the critical role of joint design, bearing material selection, and parametric sizing in ensuring functional performance and durability. Comprehensive system-level descriptions of tie rod assemblies highlight the use of thermoplastic bearing materials such as polyoxymethylene (POM) and PEEK, as well as sealing strategies and design criteria governing load capacity and service life [2]. Parametric design approaches have further enabled durability-driven sizing of ball joints to achieve infinite fatigue life [3]. Fundamental joint behavior, including the influence of clearance, lubrication, and friction on dynamic response, has also been investigated [4]. Fatigue life prediction and experimental validation studies have underscored the sensitivity of ball joint performance to stress distribution [5]. More recently, it has been shown that reduced bearing race thickness significantly increases deformation and contact stress, reinforcing the importance of stiffness and contact mechanics in joint stability [6].

Several studies have examined failure mechanisms and reliability concerns in tie rods and ball joints under service loading. Fatigue has been identified as the dominant failure mode in tie rod ends and ball joints, often initiated at stress concentration regions and exacerbated by improper processing conditions [7,8]. Reliability-oriented methods such as failure mode, effects, and criticality analysis (FMECA) have been applied to steering tie-rod joints to assess safety implications of joint degradation [9]. Reliability-based testing strategies and statistical evaluation of tie-rod joint failures further emphasize the importance of durability validation under realistic operating conditions [10].

Numerous studies have explored the lightweighting of tie rods through material substitution and structural optimization. Significant weight reductions have been demonstrated by replacing steel with aluminum alloys and applying metamodel-based optimization while maintaining durability and buckling performance [11,12]. Topology optimization techniques have also been used to improve outer tie rod shaft designs under

buckling and fatigue constraints [13]. Other investigations have focused on geometry and material modifications to reduce mass while preserving structural integrity [14,15]. These studies primarily address global structural optimization rather than joint-level manufacturing effects.

Finite element-based studies have been widely used to evaluate the structural behavior of tie rods under operational loading. Stress distribution, deformation, vibration behavior, and natural frequencies of tie rod assemblies have been analyzed using detailed FE models [16–19]. While these works provide valuable insight into global structural performance, they generally do not address joint-level behavior or the influence of manufacturing parameters on functional performance.

Broader studies on automotive lightweighting and sustainability emphasize material efficiency, energy reduction, and environmental impact. Reviews of advanced lightweight materials and manufacturing strategies highlight approaches aimed at reducing vehicle mass, energy consumption, and emissions, providing contextual motivation for component-level weight reduction studies [20–22].

Other studies have addressed automotive lightweighting and performance improvement through system-level optimization, advanced materials, and component-specific design. Multiobjective optimization frameworks integrating CAD, CAE, and multibody dynamics have been shown to significantly improve suspension system performance while reducing mass and stress levels [23]. In parallel, material-focused studies highlight the role of advanced aluminum alloys and microstructure control in achieving improved strength-to-weight ratios and durability [24], driven by fuel economy and emission reduction targets [25]. At the component level, several works have investigated tie rod optimization through material substitution, geometric modification, and topology optimization to reduce weight while maintaining structural integrity [26–30]. Finite element-based analyses have further explored stress, vibration, fatigue, and shear failure behavior of tie rods under realistic loading conditions [31,32]. Manufacturing-oriented lightweight design strategies and forming technologies provide additional context for enabling mass reduction without compromising performance [33]. The wear intensity of the ball stud and bearing in the tie rod end was calculated in a study where real-world vehicle steering was modeled [34].

Although prior research has extensively explored tie rod lightweighting through material substitution, structural optimization, and numerical modeling of ball joint mechanics and fatigue, the combined effects of manufacturing parameters—specifically pressing force, tempering method, and tempering temperature—on the functional and durability performance of reduced-diameter ball joints remain insufficiently understood. In particular, hands-on experimental studies directly linking these process variables to articulation torque, axial displacement, and stiffness under both wear and thermo-mechanical loading are scarce. Addressing this gap, the present study conducts a systematic, industrial-scale experimental investigation under realistic production conditions to evaluate the feasibility of reducing the inner tie rod ball diameter. The results provide practical, process-level insights that support the development of lighter, cost-effective, and durable steering components

while maintaining compliance with automotive performance and safety standards, contributing to broader lightweighting and sustainability objectives.

## 2. Materials and methods

The materials used in the inner tie rod assembly are first introduced. Then, the study details its characteristics and production methods before arranging test samples to evaluate the key parameters of the tempering method, tempering temperature, and press force.

### 2.1. Materials

The inner tie rod assembly consists of three main components: the ball stud, housing, and ball race, each made from specific materials to meet performance requirements. The housing is made from C15 steel, in compliance with EN 10277-2 [35], and undergoes case hardening. It is externally manufactured through cold forging. The ball stud is produced from 30MnVS6 steel, a micro-alloyed material specified by DIN EN 10267. Manufactured via cold forging, this process eliminates the need for post-forging heat treatment, resulting in cost advantages. The ball race is made of POM, a plastic material commonly used in inner tie rod ball joints due to its exceptional durability, high crystallinity, and thermoplastic properties. POM offers excellent performance, including high strength, stiffness, and toughness, with minimal water absorption [36].

The initial tie rod diameter was set at  $\text{Ø}29$  mm, matching the reference design. The target ball size is  $\text{Ø}26$  mm. The key dimensions of the  $\text{Ø}29$  ball stud and its housing are illustrated in **Figures 2** and **3**, respectively. The production and testing of the inner tie rods were carried out in the labs of a private company in Türkiye.

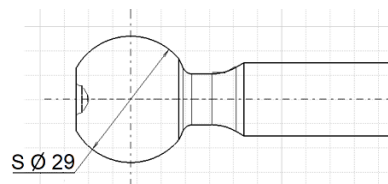


**Figure 2.** Inner tie rod ball stud.

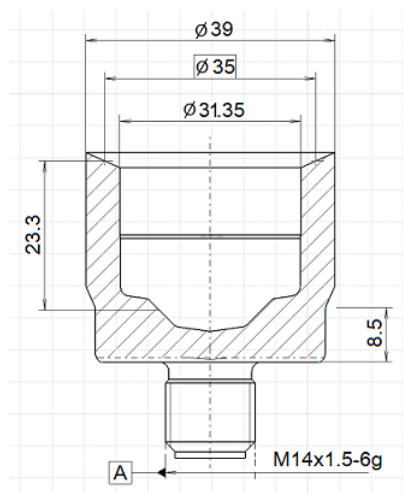


**Figure 3.** Housing of the inner tie rod.

## 2.2. Assembly procedure

Inner tie rod assemblies were produced following a controlled three-step assembly sequence, as illustrated in **Figure 4**. First, the POM ball race was inserted into the steel housing. This was followed by the insertion of the ball stud into the housing, after which the complete assembly was consolidated by axial pressing using a hydraulic press. To investigate the influence of assembly force on functional performance, three pressing force levels were employed: the minimum press force (MPF) of 120 kN, MPF + 10 kN, and MPF + 20 kN.

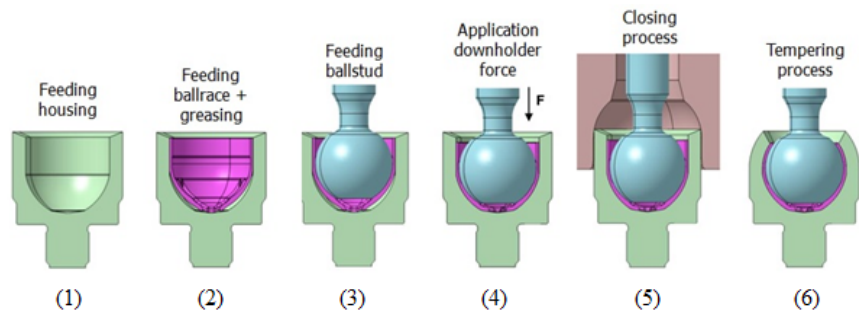


**Figure 4.** Steps of the assembly process.

## 2.3. Tempering procedure

Tempering is applied after assembly to stabilize ball–race contact and reduce articulation torque. Without tempering, ball joints experience excessive friction and high torque. To achieve optimal performance, two methods are used: oven tempering and ball tempering. The temperature and duration must be precisely controlled according to the inner tie rod’s functional requirements.

### 2.3.1. Oven tempering

In oven tempering, the fully assembled inner tie rod is heated to 145 °C or 155 °C using an electric oven rated at 160 °C and 55 kW. Assemblies are placed on open-frame carts to ensure uniform airflow and heat transfer. This process stabilizes ball–race contact but heats the entire assembly, including nonessential parts, which increases energy consumption without affecting the ball stud.

### 2.3.2. Ball tempering

Ball tempering focuses exclusively on heating the spherical ball stud to 145 °C for a controlled period before insertion. Unlike oven tempering, this method preheats only the ball between the second and third assembly steps, ensuring the required articulation torque values are achieved. By targeting the critical contact area directly, ball tempering eliminates the need for full-assembly oven heating and reduces overall energy consumption.

## 2.4. Test sample design

The experimental study was designed to evaluate whether the ball diameter of an inner tie rod assembly could be reduced without compromising functional performance or durability. In total, 192 inner tie rod assemblies were manufactured, comprising 12 reference samples with a Ø29 mm ball diameter and 180 samples

with a reduced Ø26 mm ball diameter. The Ø29 mm reference group was produced under customer-approved manufacturing conditions and served as the baseline against which all reduced-diameter configurations were assessed. The Ø26 mm design was subsequently investigated through a controlled parametric study in which the key manufacturing variables—pressing force, tempering method, and tempering temperature—were systematically varied to assess their individual and combined effects on joint performance.

For each parameter combination, a batch of 12 assemblies was produced. Each assembly was tested using three repeated measurements, and the reported results represent mean values with corresponding standard deviations, ensuring statistical consistency and reliability. The experimental program followed a sequential, industry-oriented screening and validation workflow. First, all assemblies underwent baseline functional testing, including axial travel ( $S_a$ ), minimum axial stiffness ( $C_{a,min}$ ), and articulation torque ( $M_t$ ). These pre-test measurements were evaluated against the AK-LH-14 acceptance criteria to identify viable process windows. Parameter sets failing to meet any acceptance limit at this stage were excluded from further testing, as they were considered unsuitable for series production. Only configurations that fully satisfied all pre-test functional requirements were subsequently advanced to durability testing, consisting of wear and setting tests to assess long-term and thermo-mechanical performance. This stepwise screening strategy reflects standard industrial validation practice by prioritizing functional compliance prior to durability assessment, minimizing unnecessary testing of non-viable configurations, and enabling systematic identification of robust manufacturing conditions. The functional implications of the selected parameters and the reasons for excluding specific sets are discussed in detail in the Results and Discussion section.

## 2.5. Functional measurements

To ensure durability, safety, and performance, key functional properties of inner tie rods are measured both before and after standardized wear and setting tests, as mandated by the global AK-LH-14 standard. The acceptance criteria for these tests are detailed in **Table 1**.

**Table 1.** Acceptance criteria for functional measurements.

	Pre-testing	Post-testing
Axial (spring) travel ( $S_a$ )	max. 0.05 mm at $\pm 3$ kN	max. 0.4 mm at $\pm 3$ kN
Min. axial stiffness ( $C_{a,min}$ )	100 kN/mm	2 kN/mm
Articulation torque ( $M_t$ )	0.5–3.5 Nm	0.2–3.5 Nm

### 2.5.1. Axial (spring) travel ( $S_a$ )

The process evaluates axial movement between the joint housing and ball race by applying a force of  $\pm 3$  kN, where the resulting axial travel of the ball stud must not exceed a maximum allowable limit, measured using the apparatus shown in **Figure 5**.

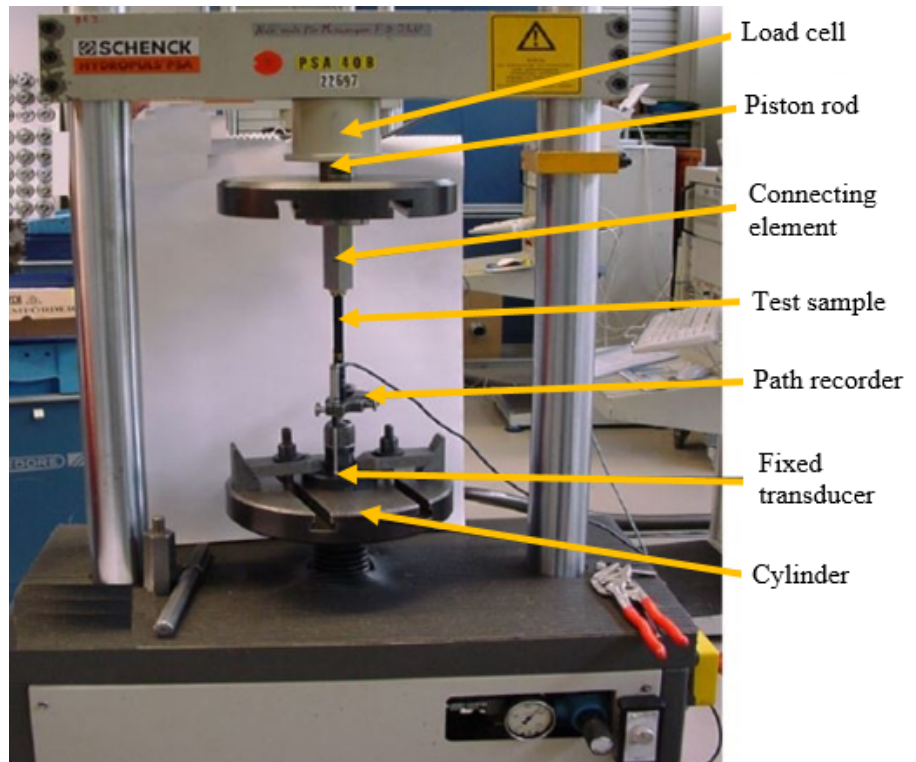


**Figure 5.** Axial travel recording apparatus.

### 2.5.2. Minimum axial stiffness ( $C_{a,min}$ )

Minimum axial stiffness is defined as the smallest tangent slope in the linear section of a joint's load-displacement curve, determined by calculating the gradient between two points on the flattest portion of the curve.

### 2.5.3. Articulation (tilting) torque ( $M_t$ )

Articulation torque, which measures the sliding friction within a joint after its initial breakaway movement, is conditioned by first articulating the ball stud five times to ensure uniform grease distribution, and is then measured over five cycles of  $\pm 22^\circ$  articulation at  $10^\circ/s$ , as illustrated in **Figures 6 and 7**.

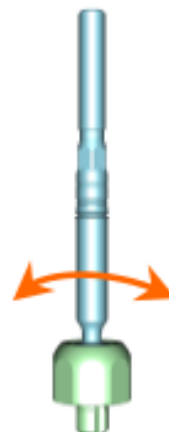


**Figure 6.** Articulation torque.

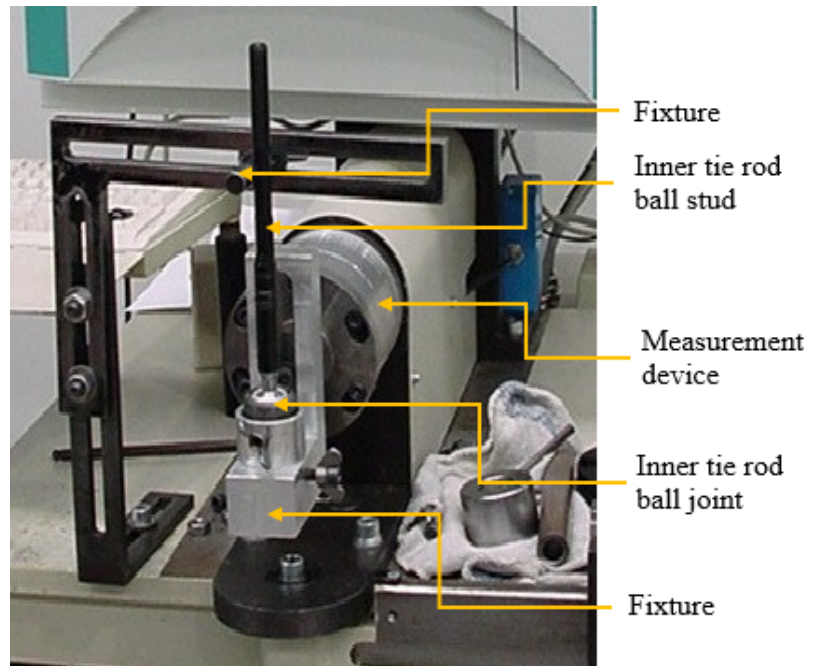


**Figure 7.** Articulation torque recording apparatus.

### 2.6. Setting test

The setting test evaluates the deformation behavior of inner tie rods under combined mechanical loading and elevated temperature. It focuses on assessing the ability of the plastic bearing to maintain structural integrity and alignment when subjected to maximum expected service loads. The maximum assist force is determined from strain-gauge measurements obtained on test tracks under extreme operating conditions [37]. During the test, a sinusoidal axial load of  $\pm 23$  kN is applied over three cycles while the ball joints are heated to  $80$  °C, as illustrated in **Figure 8**.

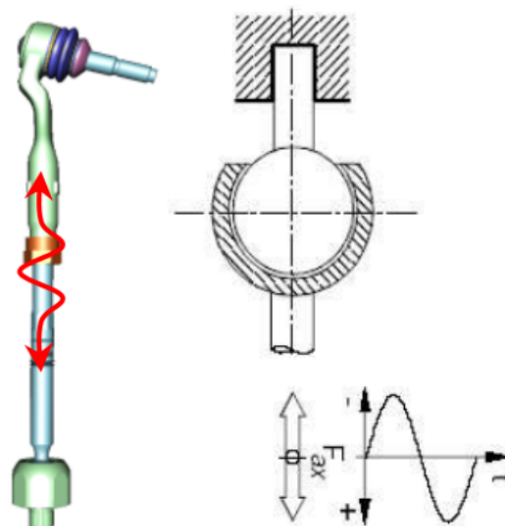


**Figure 8.** Setting test.

### 2.7. Wear test

The wear test assesses the durability and resistance to material degradation of inner tie rods under simulated operational conditions. A total of 62,500 wear cycles is applied, following the specific load phases detailed in **Table 2**. Throughout the entire test, the

component is subjected to an axial load, a constant articulation angle of 14°, and a controlled temperature of 80 °C. These elevated conditions are designed to accelerate wear, particularly in the POM material, thereby enabling the reliable prediction of the component’s long-term performance and service life in the vehicle.

**Table 2.** Wear test cycle phases.

Test load [kN]	Frequency [Hz]	Cycle
±8885	2	1250
±7626	4	2500
±5724	4	2500
±4464	2	6250
±3276	1	25,000
±2468	2	25,000

### 3. Results and discussion

After the initial functional screening, selected configurations were subjected to durability testing to evaluate wear behavior and thermo-mechanical stability. For each selected configuration, specimens were divided equally between wear and setting tests to independently assess friction-related degradation and temperature-assisted deformation.

For the Ø26 mm ball design, pressing force was increased stepwise to define a robust manufacturing window. This incremental approach enabled the elimination of unstable parameter combinations and supported the selection of process conditions that met both functional and durability requirements, confirming the feasibility of the reduced ball diameter for series production.

Prior to durability testing, all assemblies were characterized by articulation torque and minimum axial stiffness measurements, which were repeated after wear and setting tests to verify compliance with performance criteria. Based on these evaluations, representative parameter sets were selected and relabeled as Batches 1–4, as shown in **Figure 9**, with the corresponding pressing force, tempering method, and tempering temperature summarized in **Table 3**.

As illustrated in **Figure 9**, Groups 1 and 2 employed oven tempering, while Group 3 used ball tempering. In Group 1, all parameter sets were eliminated due to excessive axial travel or articulation torque exceeding acceptance limits. Increasing the tempering temperature in Group 2 by +10 °C resulted in a stable configuration that met all functional requirements and was selected for durability testing (Batch 2). In Group 3, most parameter sets satisfied pre-test requirements; two representative sets were selected to capture the performance range (Batches 3 and 4).

Comparison of Batches 1 and 2 demonstrates that articulation torque is highly sensitive to tempering temperature for the Ø26 mm design. At the initial tempering temperature, insufficient softening of the POM ball race limited surface conformity to the steel ball, resulting in elevated torque due to increased contact pressure and friction. Increasing the tempering temperature by +10 °C improved the viscoelastic deformation of the POM material, reduced torque to acceptable levels, and compensated for process-related heat losses during handling. This temperature adjustment, therefore,

represents a practical and robust solution aligned with industrial production conditions.

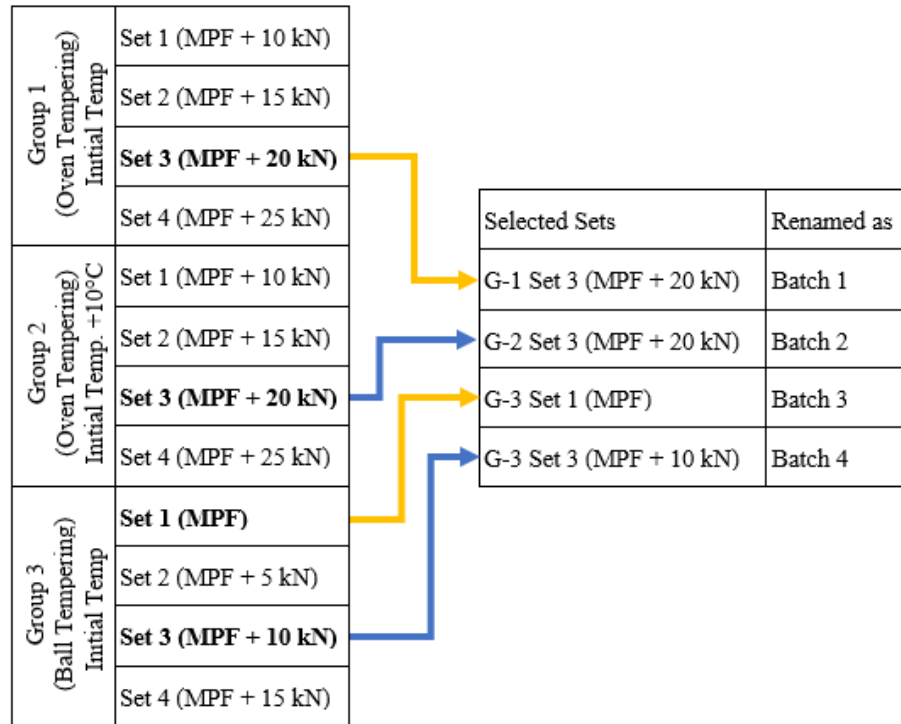


**Figure 9.** Test set arrangement.

**Table 3.** Inner tie rod sample sets.

Batch No.	Pressing force	Tempering method	Tempering temperature
1	MPF + 20 kN	Oven	Initial
2	MPF + 20 kN	Oven	Initial + 10 °C
3	MPF	Ball	Initial
4	MPF + 10 kN	Ball	Initial

This behavior indicates that the initial tempering temperature was insufficient to promote adequate viscoelastic softening of the POM ball race, limiting its ability to plastically conform to the steel ball during assembly and resulting in elevated articulation torque. Increasing the tempering temperature by +10 °C enhances material softening and surface conformity, thereby reducing localized contact pressure and friction. From an industrial perspective, this temperature increase also compensates for unavoidable heat losses during handling and transfer of components from the tempering furnace to subsequent assembly stages. Consequently, the selected +10 °C adjustment reflects both material behavior and realistic production conditions.

### 3.1. Test results of Ø29 ball size

The Ø29 mm reference design (Batch 0) was evaluated to establish a baseline for the reduced ball joint. All functional parameters ( $S_a$ ,  $C_{a,min}$ , and  $M_t$ ) satisfied the AK-LH-14 requirements. Wear tests (samples 29-0-1 to 29-0-6) and setting tests (samples 29-0-7 to 29-0-12) were conducted, with results summarized in **Figures 10** and **11**. Bars represent mean values with standard deviations, while blue and orange markers denote pre- and post-test measurements and acceptance limits, respectively.

Note that for axial travel ( $S_a$ ), values must remain below the specified limit lines; for minimum axial stiffness ( $C_{a,min}$ ), values must exceed the specified limit lines; and for articulation torque ( $M_t$ ), values must fall between the defined upper and lower limit lines.

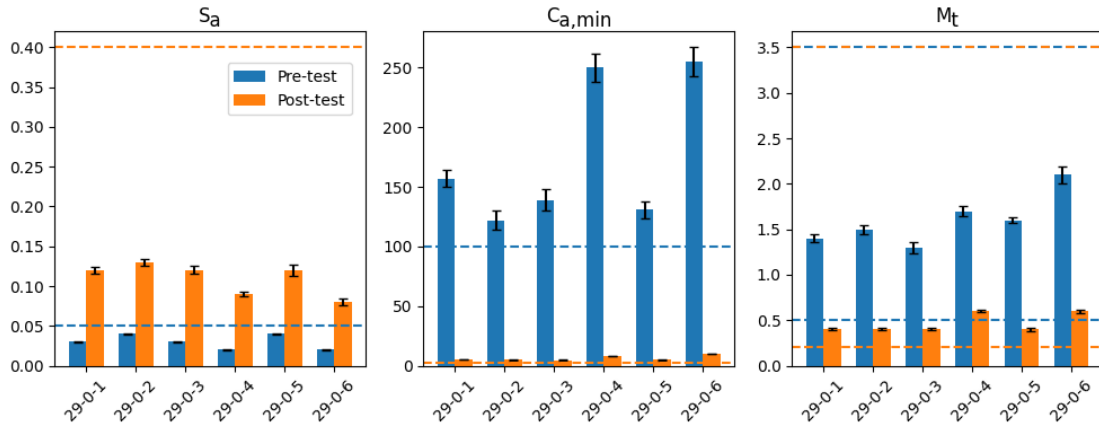


**Figure 10.** Functional measurements of Ø29 inner tie rod samples from Batch 0 before and after wear test.

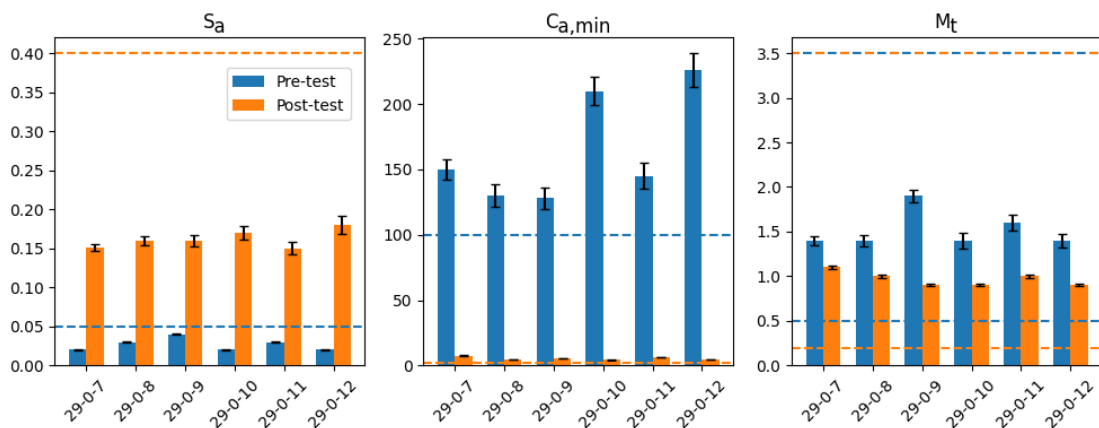


**Figure 11.** Functional measurements of Ø29 inner tie rod samples from Batch 0 before and after setting the test.

As shown in **Figure 10**, wear testing increased axial travel and reduced minimum axial stiffness and articulation torque due to plastic race wear and reduced friction; however, all pre- and post-test values remained within acceptance limits.

**Figure 11** shows similar trends after the setting test, with increased axial travel and reduced articulation torque and stiffness relative to pre-test values due to thermo-mechanical deformation of the plastic bearing under elevated temperature and loading, as well as reduced friction from surface wear; nevertheless, all post-test values remained within the acceptance limits.

### 3.2. New small-diameter axial bearing design

#### 3.2.1. Oven tempering test results

For Batch 1, the samples were produced using a pressing force of “MPF + 20 kN” and oven tempering at the “initial” temperature. As shown in **Figure 12**, samples

26-1-1, 26-1-5, and 26-1-6 failed to meet the articulation torque requirement prior to the setting test (marked by red X). Although these samples satisfied the acceptance criteria after testing, they were classified as unacceptable due to their pre-test noncompliance; therefore, wear testing was not performed. These results indicate that, under the initial tempering condition, the applied press force is either excessive or the tempering temperature is insufficient to ensure acceptable articulation torque before durability testing.

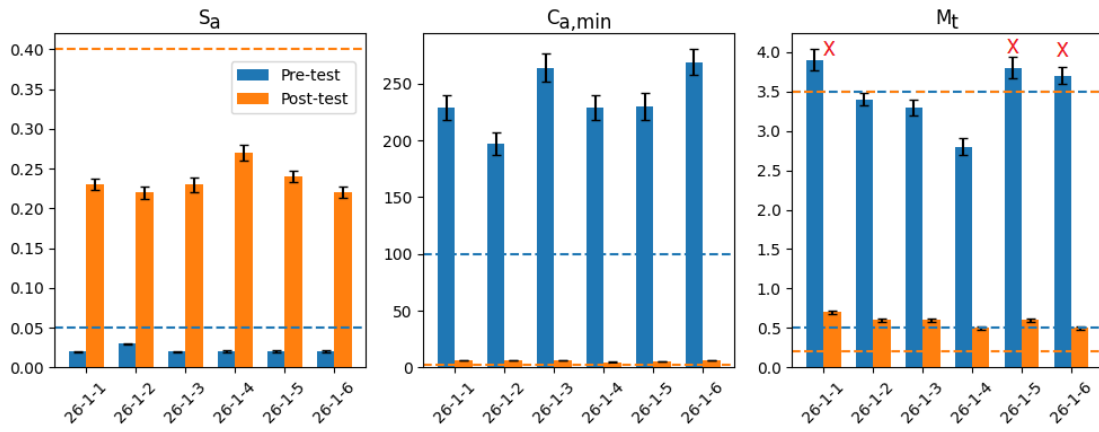


**Figure 12.** Functional measurements of Ø26 inner tie rod samples from Batch 1 before and after the setting test.

Batch 2 was produced using the same pressing force (MPF + 20 kN) as Batch 1, with the tempering temperature increased by +10 °C to achieve acceptable pre-test articulation torque. As shown in **Figures 13** and **14**, the elevated tempering temperature effectively reduced articulation torque compared to Batch 1, bringing the pre-test values closer to the specified limits. Although pre-test torque values for the wear test remained near the upper limit, they were consistently lower than those observed in Batch 1, confirming that the temperature increase provided the desired torque reduction without altering the press force. Post-wear test results, as well as pre- and post-test measurements from the setting test, remained within the acceptance criteria.

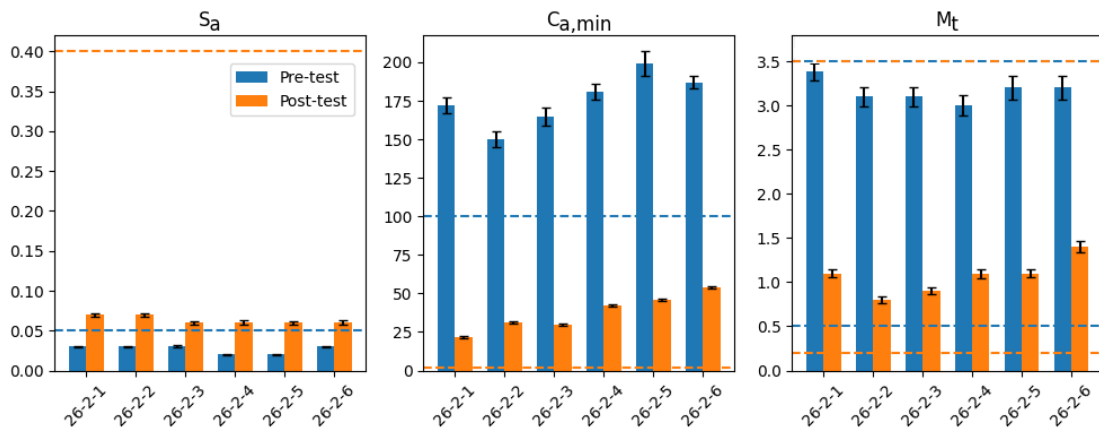


**Figure 13.** Functional measurements of Ø26 inner tie rod samples from Batch 2 before and after the wear test.

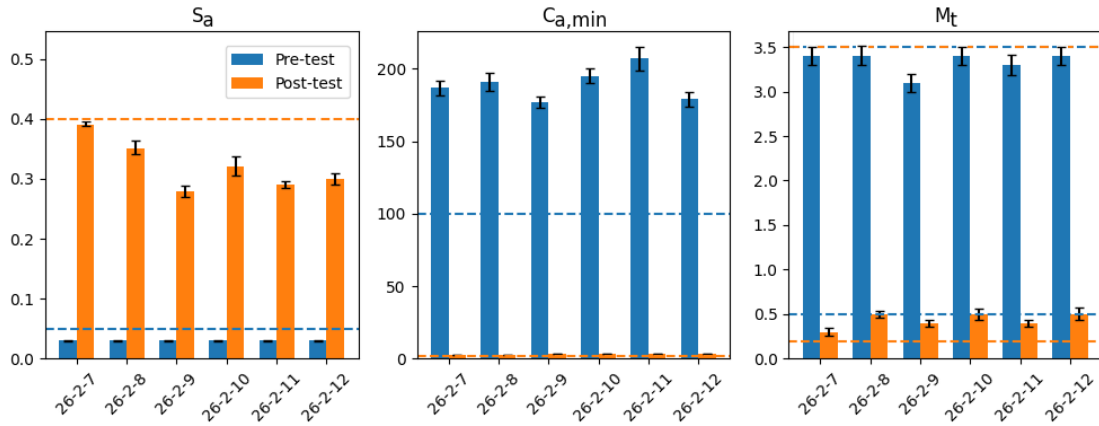


**Figure 14.** Functional measurements of Ø26 inner tie rod samples from Batch 2 before and after the setting test.

Accordingly, it is concluded that for Ø26 ball joint production, a pressing force of MPF + 20 kN combined with an oven tempering temperature of Initial + 10 °C satisfies the AK-LH-14 requirements and is suitable for series production.

### 3.2.2. Ball tempering test results

Batch 3 samples were produced using ball tempering with an MPF press force. As shown in **Figures 15** and **16**, both pre- and post-wear test measurements satisfied the specified acceptance criteria, and pre-test measurements for the setting test were within allowable limits. However, following the setting test, axial travel (Sa) exceeded the allowable limits and minimum axial stiffness (Ca,min) dropped below the acceptance threshold in five out of six samples, rendering the majority of the batch unacceptable.

The results indicate that although the reduced press force effectively lowers internal stresses and improves pre-test articulation torque (Mt), it provides insufficient resistance to thermo-mechanical loading during the setting test. Excessive deformation of the plastic ball race under elevated temperature and load leads to increased axial travel and reduced stiffness. Therefore, while ball tempering combined with MPF press force improves initial torque performance, relying solely on MPF press force is not sufficient to ensure dimensional stability and functional robustness for series production.

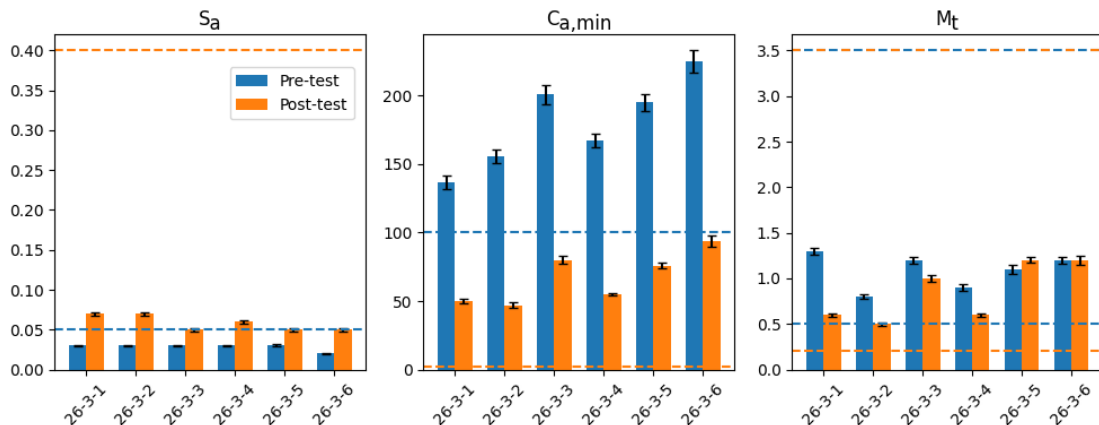


**Figure 15.** Functional measurements of Ø26 inner tie rod samples from Batch 3 before and after the wear test.

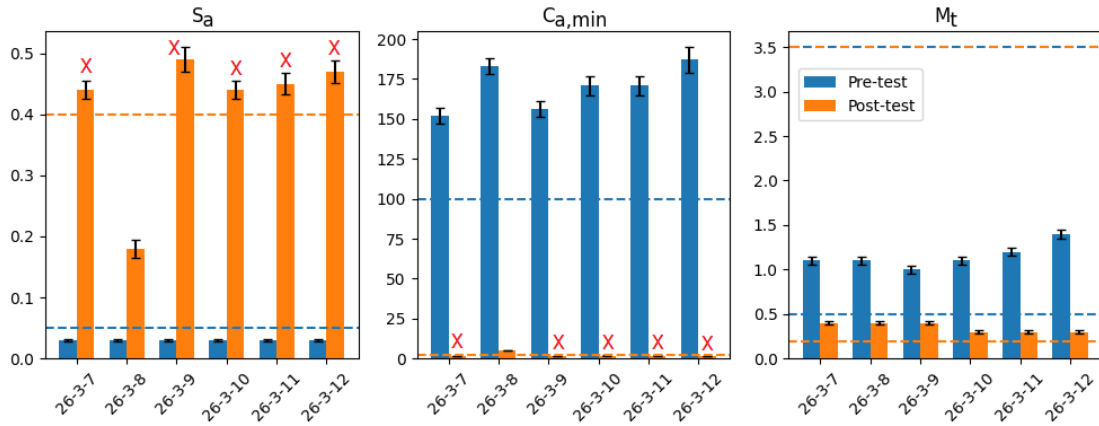


**Figure 16.** Functional measurements of Ø26 inner tie rod samples from Batch 3 before and after the setting test.

As shown in **Figures 17 and 18**, Batch 4 samples produced with an increased press force exhibited improved pre-test articulation torque, while all wear test measurements satisfied the specified acceptance criteria. In addition, both pre- and post-test results from the setting test remained within allowable limits, confirming compliant functional performance across all evaluated parameters.

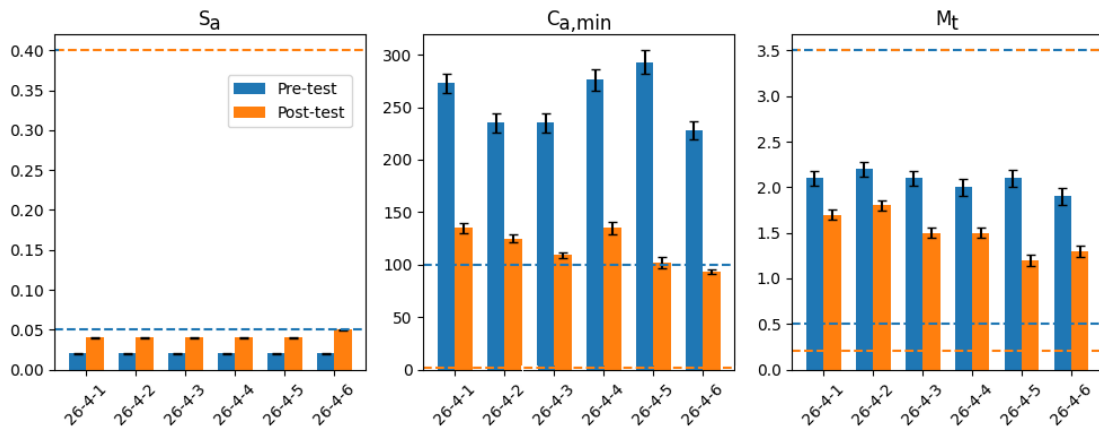


**Figure 17.** Functional measurements of Ø26 inner tie rod samples from Batch 4 before and after the wear test.

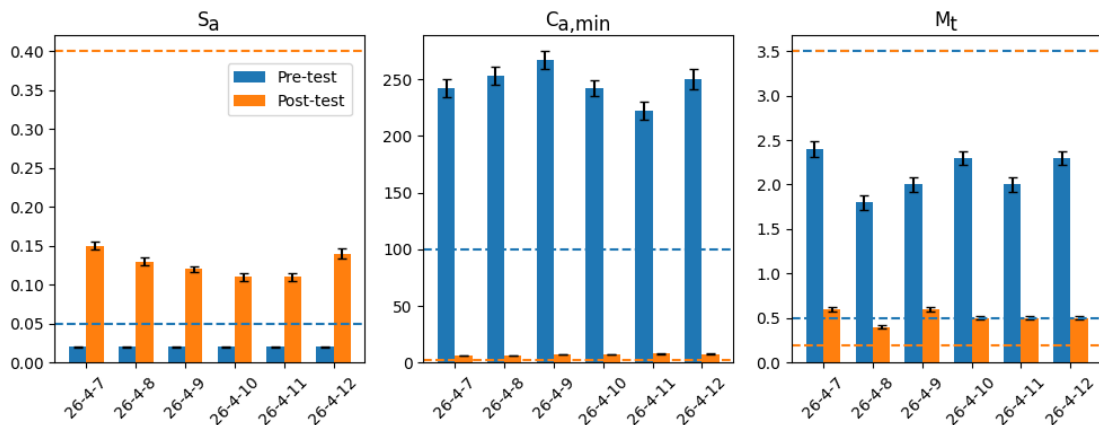


**Figure 18.** Functional measurements of Ø26 inner tie rod samples from Batch 4 before and after the setting test.

The improved performance observed in Batch 4 indicates that the increased press force effectively enhances joint stability by reducing susceptibility to deformation under wear and thermo-mechanical loading. Unlike Batch 3, the higher press force provides sufficient resistance to maintain axial travel and stiffness within acceptable limits, demonstrating that this configuration offers a robust and production-ready solution that meets all required standards.

Consequently, the results demonstrate that for Ø26 ball joint production, a pressing force of MPF + 10 kN combined with an initial ball tempering temperature satisfies the AK-LH-14 [1] requirements and provides a viable solution for series production.

A comparative evaluation of the tested batches highlights the role of both tempering temperature and pressing force in achieving robust functional performance. In Batch 1, excessive pre-test articulation torque prevented progression to wear testing, indicating that the initial tempering temperature was insufficient under the applied press force. Increasing the tempering temperature by +10 °C in Batch 2 successfully reduced pre-test torque to acceptable levels, enabling both wear and setting tests to be completed; the favorable post-test results confirmed the suitability of this configuration.

Batch 3 demonstrated that ball tempering combined with a lower press force can achieve acceptable pre-test torque and wear performance; however, the pronounced degradation observed after the setting test revealed insufficient resistance to thermo-mechanical loading, resulting in excessive axial displacement and stiffness loss. This outcome underscores the limitation of relying solely on reduced press force for stability.

In contrast, Batch 4 showed that combining ball tempering with an increased press force restores dimensional stability under both wear and setting conditions. All functional parameters remained within acceptance limits before and after testing, confirming that this configuration provides a robust and production-ready solution. Collectively, these findings emphasize the need to balance tempering strategy and press force to ensure both initial compliance and long-term durability in reduced-diameter ball joint designs.

The results show that reducing inner tie rod ball diameter is not a purely geometric scaling problem; functional stability is governed by the interaction between manufacturing parameters and joint contact mechanics. Prior work has largely emphasized lightweighting via material substitution and structural/topology optimization [11–13, 19–21] or simulation-driven sizing methodologies for ball joints [3], but these approaches typically do not resolve the strong process sensitivity observed at the joint/bearing interface under series-representative conditions.

Ball tempering localized heat input and is therefore attractive from an energy/process-efficiency standpoint; however, the durability response indicates that tempering strategy alone is insufficient when press force is minimized. Although wear-stage results remained acceptable, setting tests produced excessive axial travel and stiffness loss, indicating thermo-mechanical deformation of the polymer bearing under combined temperature and load. This failure mode aligns with fatigue/reliability studies showing that joint performance and life are highly sensitive to stress distribution, preload, and local damage evolution [5,7,8], and is consistent with tribological evidence that polymer

contact behavior depends strongly on frictional and wear conditions [36]. Increasing press force in the ball-tempered configuration mitigated deformation and stabilized post-setting performance, indicating that adequate preload is required to maintain joint dimensional stability once bearing compliance is reduced.

The study establishes that robust Ø26 performance requires a balanced combination of tempering method and press force, rather than material change or geometry optimization alone. By providing industrial, hands-on validation beyond simulation-centric studies [3,11–13], the results help translate lightweighting objectives into a production-ready process window while maintaining compliance with steering joint performance and durability requirements [1,2,37].

The energy- and cost-related implications discussed in this study are subject to several boundary conditions and sources of uncertainty that should be considered when interpreting the results. The experimental campaign focused on functional and durability performance, and direct measurements of energy consumption during pressing and tempering operations were not performed. Consequently, energy-related comparisons are based on relative process indicators, including ball diameter, heated mass, tempering temperature level, and tempering strategy, rather than absolute energy values. Variability in furnace efficiency, batch loading, heating duration, and heat losses during component handling and transfer between process steps may influence the actual energy consumption in a production environment. In addition, press force variations and cycle times are assumed to remain within typical industrial tolerances for series production. These assumptions reflect realistic manufacturing conditions but introduce uncertainty when extrapolating results to different production lines or equipment configurations. Accordingly, the energy efficiency and cost discussions are intended as comparative, process-level assessments, highlighting trends and potential benefits rather than precise quantitative savings. Future work, including direct energy monitoring and line-specific data, would enable a more detailed evaluation of absolute energy and cost impacts.

#### **4. Conclusion**

This study demonstrates that reducing the inner tie rod ball diameter from Ø29 mm to Ø26 mm is feasible without compromising compliance with AK-LH-14 functional and durability requirements, provided that manufacturing parameters are appropriately optimized. Experimental results show that articulation torque, axial displacement, and minimum axial stiffness are highly sensitive to pressing force and tempering strategy, with this sensitivity becoming more pronounced as ball diameter is reduced. In particular, articulation torque was identified as the most critical parameter governing pre-test acceptance.

Ball-tempered designs produced with minimum press force achieved acceptable initial torque and wear performance, but failed under setting conditions due to excessive axial deformation and stiffness loss. By contrast, combining ball tempering with an increased press force (MPF + 10 kN) resulted in stable functional behavior before and after both wear and setting tests, satisfying all acceptance criteria.

Unlike simulation-driven studies, this work provides industrial-scale, hands-on

experimental evidence that successful ball diameter reduction depends on balanced process-level optimization rather than geometric redesign alone. The validated Ø26 mm configurations offer a production-ready solution that enables material and weight reduction while limiting additional thermal input, thereby supporting cost efficiency, energy-conscious manufacturing, and sustainability objectives within existing automotive steering system production lines.

**Author contributions:** SD contributed to the conceptualization and methodology, performed the experimentation, wrote the original draft, and provided resources. MÇ contributed to the conceptualization, supervised the work, wrote the original draft, reviewed and edited the manuscript, and was a major contributor to the study. Both authors have read and agreed to the published version of the manuscript.

**Funding:** No funding was received.

**Institutional review board statement:** Not applicable.

**Informed consent statement:** Not applicable.

**Data availability statement:** Comprehensive measurement results, including detailed performance data for all assemblies, are available from the corresponding author upon reasonable request.

**Conflict of interest:** The authors declare no conflict of interest.

## References

1. AK-LH 14. Suspension joints/requirements and testing. Working Committee Specification Book; 2004.
2. Adamczyk D, Kleiner W, Maehlmann D. Tie rods. In: Harrer M, Pfeffer P (editors). *Steering Handbook*. Springer International Publishing; 2017. pp. 339–356. doi: 10.1007/978-3-319-05449-0\_12
3. Geren N, Akçalı OO, Unver E, et al. Automated sizing of automotive steering ball joints in a parametric CAD environment using expert knowledge and feature-based computer-assisted 3D modelling. *Advanced Engineering Informatics*. 2022; 52: 101630.
4. Flores P, Ambrósio J, Claro JCP, et al. A study on dynamics of mechanical systems including joints with clearance and lubrication. *Mechanism and Machine Theory*. 2006; 41(3): 247–261. doi: 10.1016/j.mechmachtheory.2005.10.002
5. Uguz A, Oka SH. Modeling the effects of mechanical loads: Finite element modeling of ball joints under dynamic loading. *Materials Testing*. 2004; 46(10): 506–512.
6. Mose BR, Shin DK, Nam JH. Numerical analysis of stresses on angular contact ball bearing under static loading with respect to race thickness and housing stiffness. *Scientific Reports*. 2024; 14: 16673. doi: 10.1038/s41598-024-66479-y
7. Falah AH, Alfares MA, Elkholy AH. Failure investigation of a tie rod end of an automobile steering system. *Engineering Failure Analysis*. 2007; 14(5): 895–902. doi: 10.1016/j.engfailanal.2006.11.045
8. Burcham MN, Escobar R, Yenusah CO, et al. Characterization and failure analysis of an automotive ball joint. *Journal of Failure Analysis and Prevention*. 2017; 17: 262–274. doi: 10.1007/s11668-017-0240-4
9. Ćatić D, Jeremić B, Djordjević Z, et al. Criticality analysis of the elements of the light commercial vehicle steering tie-rod joint. *Strojniški Vestnik—Journal of Mechanical Engineering*. 2011; 57(6): 495–502. doi: 10.5545/sv-jme.2010.077
10. Ćatić D, Krstić B, Miloradović D. Determination of reliability of motor vehicle steering system tie-rod joint. *Journal of the Balkan Tribological Association*. 2009; 15(3): 309–322.
11. Kim JK, Kim YJ, Yang WH, et al. Structural design of an outer tie rod for a passenger car. *International Journal of Automotive Technology*. 2011; 12(3): 375–381. doi: 10.1007/s12239-011-0044-6
12. Park YC, Baek SK, Seo BK, et al. Lightweight design of an outer tie rod for an electric vehicle. *Journal of Applied*

- Mathematics. 2014; 2014(4): 942645.
13. Mete E, Başak H. Outer tie rod design by using topology optimization, analysis and verification. *Journal of Polytechnic*. 2024; 27(3): 1055–1068.
  14. Navale P, Katekar S. Optimization of car tie rod with the help of finite element analysis. In: *Proceedings of the 4th International Conference on Advanced Technologies for Societal Applications (Techno-Societal 2022)*; 9–10 December 2022; Pandharpur, India. doi: 10.1007/978-3-031-34648-4\_40
  15. Essienubong IA, Owunna I, Eburnilo PO. Design of a low alloy steel vehicle tie rod to determine the maximum load that can resist failure. *Journal of Robotics, Computer Vision and Graphics*. 2016; 1(1): 1–11.
  16. Aravindaraj E, Natrayan L, Santhosh MS, et al. Design and analysis of connecting tie rod assembly for automotive application. *Journal of Engineering Sciences*. 2018; 5(2): D15–D20.
  17. Özsoy M, Pehlivan MK. Computer aided structural analysis of a tie rod end. *Acta Physica Polonica A*. 2015; 128(2B): 488–490.
  18. Patil MA, Chavan DS, Kavade MV, et al. FEA of tie rod of steering system of car. *International Journal of Application or Innovation in Engineering and Management*. 2013; 2(5): 222–227.
  19. Gowda BS, Ravi KS, Chethan KY. Analysis and optimization of tie rod for steering mechanism of a car. *International Journal of Innovative Research in Technology*. 2016; 3(3): 61–64.
  20. Zhang W, Xu J. Advanced lightweight materials for automobiles: A review. *Materials and Design*. 2022; 221: 110994. doi: 10.1016/j.matdes.2022.110994
  21. Czerwinski F. Current trends in automotive lightweighting strategies and materials. *Materials*. 2021; 14(21): 6631. doi: 10.3390/ma14216631
  22. Giampieri A, Ling-Chin J, Ma Z, et al. A review of the current automotive manufacturing practice from an energy perspective. *Applied Energy*. 2020; 261: 114074.
  23. Llopis-Albert C, Rubio F, Zeng S. Multiobjective optimization framework for designing a vehicle suspension system: A comparison of optimization algorithms. *Advances in Engineering Software*. 2023; 176: 103375. doi: 10.1016/j.advengsoft.2022.103375
  24. Li W. Application and lightweight research of new aluminum alloy materials in automotive components. *Academic Journal of Materials and Chemistry*. 2025; 6(1), 91–99. doi: 10.25236/AJMC.2025.060111
  25. Chirinda GP, Matope S. The lighter the better: Weight reduction in the automotive industry and its impact on fuel consumption and climate change. In: *Proceedings of the 2nd African International Conference on Industrial Engineering and Operations Management*; 7–10 December 2020; Harare, Zimbabwe. pp. 520–533.
  26. Shareef MA, Dehankar RN. A literature review and study on design, fabrication and analysis of tie rods for steering mechanism. *International Journal for Research in Applied Science and Engineering Technology*. 2022; 10(5): 208–212. doi: 10.22214/ijraset.2022.41911
  27. Bhirad SS. Failure analysis and optimization of the tie rod using FEA. *International Journal for Research in Applied Science and Engineering Technology*. 2021; 9(8): 2781–2786. doi: 10.22214/ijraset.2021.37844
  28. Senniappan M, More R, Bhide S, et al. Optimization of commercial vehicle's steering tie rod arm design based on strain life approach. *SAE Technical Paper*. 2016; 2016-01-0381. doi: 10.4271/2016-01-0381
  29. Navale P, Katekar S. Validation of natural frequency for tie rod of a steering system using finite element analysis and experimental methods. *International Journal for Research in Applied Science and Engineering Technology*. 2023; 11(2): 139–154.
  30. Mungi S, Navthar R. Performance optimization of tie rod using FEA. *International Journal of Engineering Research and Development*. 2015; 11(3): 27–33.
  31. Godase AJ, Kulkarni PP, Katekar SD. Probabilistic design for strength analysis of tie rod subjected to tensile, compressive, and shear load using finite element methods. In: *Proceedings of the 2nd International Conference on Advanced Technologies for Societal Applications*; 14–15 December 2018; Pandharpur, India. doi: 10.1007/978-3-030-16962-6\_12
  32. Jia Y, Nguyen V. Evaluating automobile's vibration in frequency domain. *Mechanical Engineering Advances*. 2024; 2(1): 1239. doi: 10.59400/mea.v2i1.1239
  33. Rosenthal S, Maaß F, Kamaliev M, et al. Lightweight in automotive components by forming technology. *Automotive Innovation*. 2020; 3(3): 195–209.
  34. Wozniak M, Rylski A, Siczek K. The measurement of the wear of tie rod end components. *Strojnicki Vestnik—Journal of Mechanical Engineering*. 2022; 68(2): 101–113. doi: 10.5545/sv-jme.2021.7389
  35. European Committee for Standardization. Bright Steel Products - Technical Delivery Conditions - Part 2: Steels for

General Engineering Purposes. European Committee for Standardization; 2008.

36. Chen J, Cao Y, Li H. Investigation of the friction and wear behaviors of polyoxymethylene/linear low-density polyethylene/ethylene-acrylic-acid blends. *Wear*. 2006; 260(11–12): 1342–1348.
37. Heißing B, Ersoy M (editors). *Chassis Handbook: Fundamentals, Driving Dynamics, Components, Mechatronics, Perspectives*. Vieweg+Teubner Verlag; 2011.